

Research Article

A CCM-Based OFDM System with Low PAPR for Sparse Source

Qinbiao Yang,¹ Zulin Wang,^{1,2} and Qin Huang ¹

¹Electronic and Information Engineering, Beihang University, Beijing 100191, China

²Collaborative Innovation Center of Geospatial Technology, Wuhan 43079, China

Correspondence should be addressed to Qin Huang; qinhuang@buaa.edu.cn

Received 24 November 2017; Revised 6 February 2018; Accepted 19 February 2018; Published 21 March 2018

Academic Editor: Michael McGuire

Copyright © 2018 Qinbiao Yang et al. This is an open access article distributed under the Creative Commons Attribution License, which permits unrestricted use, distribution, and reproduction in any medium, provided the original work is properly cited.

Orthogonal frequency division multiplexing (OFDM) usually suffers high peak-to-average power ratio (PAPR). As shown in this paper, PAPR becomes even severe for sparse source due to many identical nonzero frequency OFDM symbols. Thus, this paper introduces compressive coded modulation (CCM) in order to restrain PAPR by reducing identical nonzero frequency symbols for sparse source. As a result, the proposed CCM-based OFDM system, together with iterative clipping and filtering, can efficiently restrain the high PAPR for sparse source. Simulation results show that it outperforms about 4 dB over the traditional OFDM system when source sparsity is 0.1.

1. Introduction

Due to its high-speed data rate, orthogonal frequency division multiplexing (OFDM) [1, 2] has been widely applied to the 4G mobile communication system, Wi-Fi, and some military communication systems [3–7]. However, its signals may have high peak-to-average power ratio (PAPR). Because of the nonlinearity of power amplifier (PA), it will lead to signal distortion and restrict implementation of the OFDM system [8, 9].

To solve this problem, many PAPR reduction techniques have been proposed in recent few years. These techniques can be classified into three categories [10]: multiple signaling and probabilistic techniques [11–13], coding techniques [14], and signal distortion techniques [15–19]. In general, the first two categories, that is, the multiple signaling and probabilistic techniques and coding techniques, do not increase the bit error rate (BER), but they involve high computational complexity and data rate loss [10]. Accordingly, signal distortion techniques reduce the PAPR by distorting the transmitted OFDM signal before it passes through the PA. Although signal distortion techniques slightly increase BER, they have lower computational complexity and do not result in data rate loss. Thus, in order to achieve high data rate in OFDM systems, we adopt signal distortion techniques for PAPR reduction.

In signal distortion techniques, clipping and filtering is the most popular way to reduce PAPR because of its low complexity and moderate signal distortion. It clips the OFDM signal to a predefined threshold and uses a filter to restrain the out-of-band radiation. However, the filtering operation may cause peak regrowth. Hence, iterative clipping and filtering (ICF) [15] has been proposed to suppress the peak regrowth. Some variants of ICF have been developed to increase convergence rate, for example, simplified ICF (SICF) [16], optimized ICF (OICF) [19], and simplified optimized ICF (SOICF) [20]. Only after several iterations is the SOICF able to achieve sufficient PAPR reduction with less BER degradation and low complexity.

In a traditional OFDM system, it usually takes the M-array Phase Shift Keying (MPSK) or the M-array Quadrature Amplitude Modulation (MQAM) bit-to-symbol mapping operations. If source is sparse, these bit-to-symbol mapping operations will generate more identical nonzero frequency OFDM symbols which will result in high PAPR. So PAPR becomes even severe in the case of sparse source. As a result, ICF and its variants may fail to obtain sufficient PAPR reduction.

This paper focuses on the PAPR reduction of OFDM for sparse source. The key idea to reduce PAPR for sparse source is to convert source bits into frequency OFDM symbols by

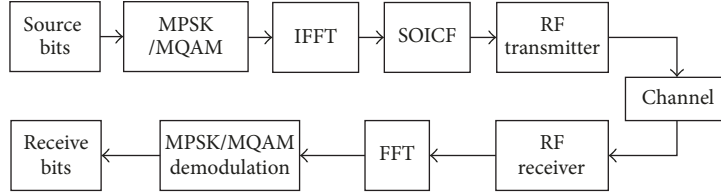


FIGURE 1: Diagram of the traditional OFDM system.

compressive coded modulation (CCM) [21] instead of traditional MPSK or MQAM. Usually, the CCM is used for seamless rate adaptation by adopting a special random projection (RP) to generate symbols from source bits. However, we verify that the RP symbols of the CCM for sparse source concentrate in zero, and there are much less nonzero symbols than those of MPSK and MQAM in the RP symbols. As a result, we propose using CCM together with SOICF to efficiently reduce the PAPR of OFDM for sparse source. Simulation results show that the proposed CCM-based OFDM system, together with the SOICF method, almost has the same performance in terms of PAPR reduction as a traditional OFDM system regardless of source sparsity. Furthermore, the proposed OFDM system outperforms about 4 dB over the traditional OFDM system when source sparsity is 0.1.

The rest of this paper is organized as follows. Section 2 briefly introduces necessary background. Section 3 presents the related theoretical analysis and the proposed novel OFDM system. Numerical and simulation results are provided in Section 4. The conclusion is given in Section 5.

2. Background

In this section, we first review the traditional OFDM system and its PAPR problem. Then, the CCM is briefly described.

2.1. Traditional OFDM System. As shown in Figure 1, a traditional OFDM system usually takes the MPSK or MQAM to convert the source bits into the frequency OFDM symbols. Then, IFFT process part generates the discrete-time OFDM signal. Furthermore, we adopt the SOICF method to restrain PAPR. Finally, the optimized signal is transmitted by the RF transmitter, which includes oversampling, upconversion, and PA. In the receiver, the source bits can be recovered by the FFT and the corresponding demodulation.

Let us define $\mathbf{b} = (b_1, b_2, \dots, b_M)^T \in \{0, 1\}$ as the source vector, where T indicates the transpose of the vector. Through the bit-to-symbol mapping operations with \mathbf{b} , the frequency OFDM symbols with N subcarriers can be written as $\mathbf{X} = [X(0), X(1), \dots, X(N-1)]$, and the discrete-time signal can be obtained by

$$\begin{aligned}
 x(n) &= \frac{1}{\sqrt{N}} \sum_{k=1}^N X(k) \cdot e^{j(2\pi nk/NL)} \\
 &= \sqrt{N} \cdot \text{IFFT}(X(k))_{NL}, \quad n = 0, 1, \dots, NL-1,
 \end{aligned} \tag{1}$$

where L is the oversampling factor and the oversampling operation is implemented by zero padding in the end of \mathbf{X} . For signal $x(n)$, the PAPR is defined as the ratio of the maximum power to the average power and can be formulated as

$$\text{PAPR} = \frac{\max\{|x(n)|^2\}}{E\{|x(n)|^2\}}, \tag{2}$$

where $E\{|x(n)|^2\}$ denotes the average power of $x(n)$. As mentioned in [22], if the elements of \mathbf{X} are statistically independent and identically distributed random variables, the real and imaginary parts of $x(n)$ are Gaussian random variables with zero mean and same variance σ^2 when $N > 64$. Consequently, the amplitude of $x(n)$, that is, $|x(n)|$, is a Rayleigh random variable and, sometimes, the peak power of $x(n)$ is much larger than its average power. In other words, it results in high PAPR of the OFDM signal, which degrades the system's performance.

2.2. CCM Scheme. The CCM scheme is a compressive coded modulation for seamless rate adaptation. Its core is a special random projection code (RPC) and the corresponding decoding algorithm. Due to the embedding of source compressive into modulation, the CCM scheme brings significant throughput gain when source is sparse. Moreover, the decoding algorithm performs joint decoding based on received RP symbols, and the number of received RP symbols can be adjusted in fine granularity. Then, it is usually used for seamless rate adaption. The key process of the CCM scheme is as follows:

- (i) Design the desired RPC.
- (ii) Use the RPC and source bits to generate the RP symbols.
- (iii) Map every two consecutive RP symbols into a wireless symbol with I and Q components.
- (iv) Transmit the wireless symbols through carrier modulation and digital-to-analog converter (DAC).
- (v) Recover the transmitted source bits through the RPC-Belief Propagation (BP) [21] decoding algorithm in the receiver.

Specifically, unlike traditional bit-to-symbol mappings, the RP can implement the bit-to-symbol mapping and channel protection at the same time. We present the schematic diagram of RP in Figure 2.

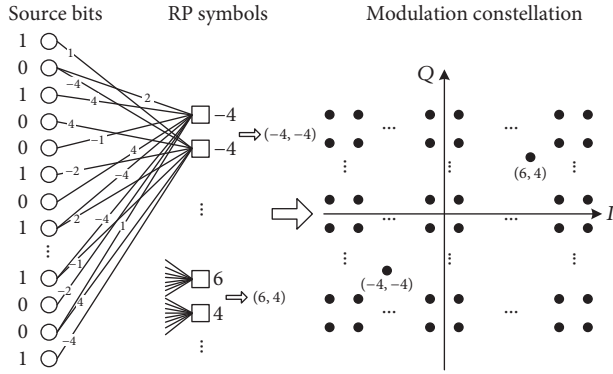


FIGURE 2: Illustration of random projection.

As illustrated in Figure 2, source bits can be converted to RP symbols by weighted sum operation. Then, every two RP symbols are mapped into one wireless symbol. Each constellation point is used to represent one wireless symbol. RPC bit-to-symbol mapping converts the source vector \mathbf{b} into a series of RP symbols s_1, s_2, \dots, s_R by weighted sum operation. Define $w = \{w_1, w_2, \dots, w_l\} \in \mathbb{Z}, l = P$, as weight set; the r th RP symbol can be generated by

$$s_r = \sum_{l=1}^P w_l \cdot b_{m_{r,l}}, \quad (3)$$

where $b_{m_{r,l}}$ is the element of the source vector \mathbf{b} and $m_{r,l}$ is the index of the bit weighted by w_l for generating symbol s_r . Based on (3), the RPC can be regarded as a low-density generator matrix \mathbf{G} . There are only P nonzero entries in every row of matrix \mathbf{G} , and w_l are located in the P columns randomly. Denote $\mathbf{s} = (s_1, s_2, \dots, s_R)^T$ as a symbol vector, and then the RP symbols can be formulated as

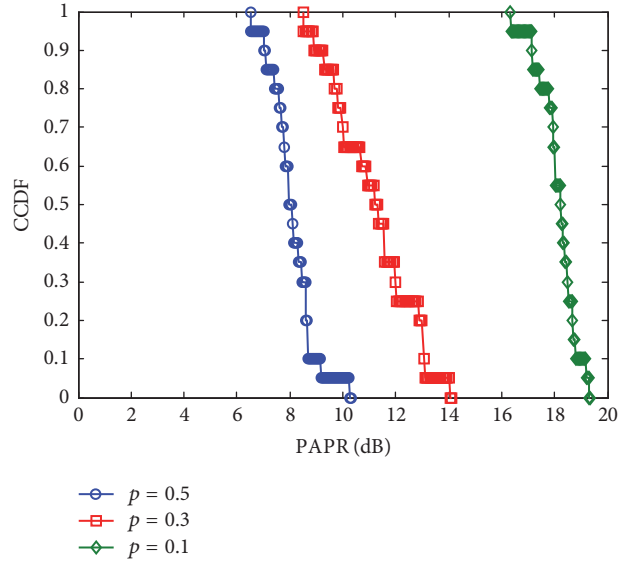
$$\mathbf{s} = \mathbf{G} \cdot \mathbf{b}. \quad (4)$$

Generally, in order to achieve better transmission rate for CCM scheme, the key problem of weight set selection is that the entropy of the RP symbols generated by the weighted sum operation is always large. In addition, the low-density characteristic of \mathbf{G} also should be guaranteed. The specific design principles of w and \mathbf{G} can be found in [21].

To generate the waveform for RF transmitter, the RP symbols have to be mapped to the amplitude of sinusoid signals. Let V_{\min} and V_{\max} be the minimum and maximum value in \mathbf{s} . Suppose that A is the maximum amplitude of sinusoid signals. The mapping is thus a linear projection from $[V_{\min}, V_{\max}]$ to $[-A, A]$, and the actual amplitude after mapping is

$$x_r = -A + \frac{2A}{V_{\max} - V_{\min}} (s_r - V_{\min}). \quad (5)$$

Eventually, the wireless symbols are transmitted to wireless channel through carrier modulation and DAC, while each wireless symbol is composed of two consecutive x_r , that is, $x_r + j \cdot x_{r+1}$.


 FIGURE 3: PAPRs for different p with QPSK-based OFDM and $L = 8$.

In the receiver, through the demodulation and inverse projection from $[V_{\min}, V_{\max}]$ to $[-A, A]$, we can obtain the noisy RP symbols from wireless channel. Furthermore, using the RPC-BP decoding algorithm, we can recover the source bits from the noisy RP symbols.

3. Proposed CCM-Based OFDM System

From Section 2.1, we know that the OFDM signal is the summation of the products of entries in \mathbf{X} and the multicarrier signals. According to (1), if some elements of \mathbf{X} have the same sign and the carriers signals have the same phase, the signal obtained by summation will have a large peak amplitude; otherwise, the signal will have a peak amplitude around the average.

The source sparsity can be modelled by unequal probabilities on the appearance of 0's and 1's [23]. In this paper, we denote the probability $P(b = 1) = p$ as the source sparsity, that is, the probability on the appearance of 1. In the traditional OFDM system, if the source sparsity p is small, that is, the source bits contain a large portion of 0's, the traditional bit-to-symbol mapping operations, for example, MPSK and MQAM, may generate a lot of identical nonzero symbols. This may cause higher PAPR than that of nonsparse source. For instance, Figure 3 shows the PAPR complementary cumulative distribution function (CCDF) [10] curves with different source sparsity. The CCDF of the PAPR denotes the probability that a PAPR exceeds a certain value. It is shown that the PAPR increases as the source becomes sparse.

The above analysis shows that the high PAPR for sparse source in traditional OFDM system is caused by the identical nonzero symbols generated by conventional bit-to-symbol mapping operations. Therefore, we would like to use new bit-to-symbol mapping that produces less identical nonzero

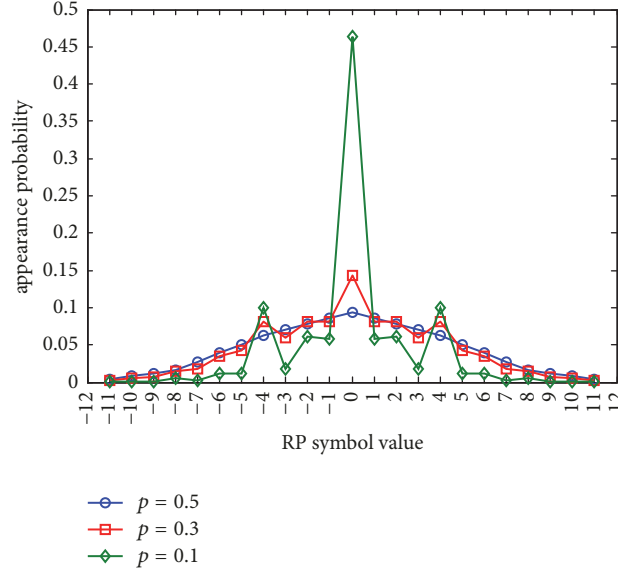


FIGURE 4: RP symbols distribution for different p .

symbols for sparse source. Later, we will verify that the CCM produces more zero symbols but less identical nonzero symbols for sparse source. This feature of the CCM promises a low PAPR for sparse source.

According to (3), we know that all the generated RP symbols are integer including zero and distribute from the minimal value to the maximal value of the sum of the weights. Moreover, the distribution of the RP symbol s_r is determined by the weight set and the source sparsity p . Considering $w = \{w_1, w_2, \dots, w_l\} \in \mathbb{Z}$, $l = P$, and $w_1 = -w_2$, $w_3 = -w_4, \dots, w_{l-1} = -w_l$, the RP symbol can be written as

$$\begin{aligned} s_r &= w_1 \cdot b_{m_{r_1}} + w_2 \cdot b_{m_{r_2}} + \dots + w_{l-1} \cdot b_{m_{r(l-1)}} + w_l \cdot b_{m_{r_l}} \\ &= w_1 (b_{m_{r_1}} - b_{m_{r_2}}) + w_3 (b_{m_{r_3}} - b_{m_{r_4}}) + \dots \\ &\quad + w_{l-1} (b_{m_{r(l-1)}} - b_{m_{r_l}}). \end{aligned} \quad (6)$$

Since the probability distribution function (PDF) of $b_{m_{r_i}}$ is

$$\begin{aligned} P(b_{m_{r_i}} = 0) &= 1 - p \\ P(b_{m_{r_i}} = 1) &= p, \end{aligned} \quad (7)$$

let b_{m_Δ} denote $(b_{m_{r(l-1)}} - b_{m_{r_l}})$; we can obtain the PDF of b_{m_Δ} as follows:

$$P(b_{m_\Delta}) = \begin{cases} p(1-p) & b_{m_\Delta} = -1 \\ p^2 + (1-p)^2 & b_{m_\Delta} = 0 \\ p(1-p) & b_{m_\Delta} = 1. \end{cases} \quad (8)$$

From (8), we can prove that $P(b_{m_\Delta} = 0)$ is always the maximal value among all values regardless of p , and the maximal value becomes large as p becomes small. That is to say, when $P = 2$, the appearance probability of zero symbol, that is, $P(s_r = 0)$, dominates the PDF of s_r . Moreover, since the PDF of s_r is a joint PDF of every b_{m_Δ} , the PDF of s_r would be similar to the case of $P = 2$ when P becomes large. For instance, if $w = \{\pm 1, \pm 2, \pm 4, \pm 4\}$, the RP symbols take value from $[-11, +11]$, and they are generated by the equation as follows:

$$\begin{aligned} s_r &= (+1) \cdot b_{m_{r_1}} + (-1) \cdot b_{m_{r_2}} + (+2) \cdot b_{m_{r_3}} + (-2) \cdot b_{m_{r_4}} \\ &\quad + (+4) \cdot b_{m_{r_5}} + (-4) \cdot b_{m_{r_6}} + (+4) \cdot b_{m_{r_7}} + (-4) \\ &\quad \cdot b_{m_{r_8}}. \end{aligned} \quad (9)$$

In Figure 4, we illustrate the RP symbols distribution for different source sparsity p .

In Figure 4, we can see that the zero symbol always dominates the distribution regardless of source sparsity p in the case of $w = \{\pm 1, \pm 2, \pm 4, \pm 4\}$. In the other cases of weight set, the same result can be obtained as Figure 4. This result also verifies the above analysis.

Therefore, the appearance probability of zero symbol always dominates the PDF of s_r regardless of p , and if p becomes small, $P(s_r = 0)$ will become large. That is to say, there are many zero symbols in RP symbols. Moreover, the sparser the source is, the more zero symbols there are.

Based on the above analysis, we use CCM together with SOICF to efficiently reduce the PAPR of OFDM for sparse source. Figure 5 illustrates the diagram of the CCM-based OFDM system.

As shown in Figure 5, we adopt the CCM scheme in the OFDM system. Then, the elements of \mathbf{X} are the RP symbols. Because the values of the RP symbols are dominated by the zero value, the large peak amplitude of the summation

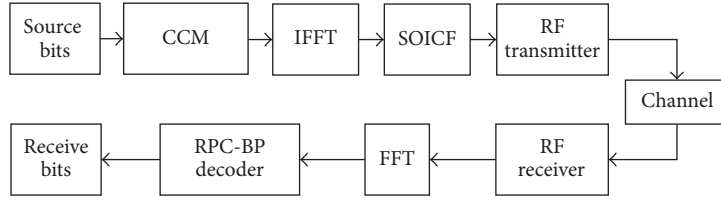
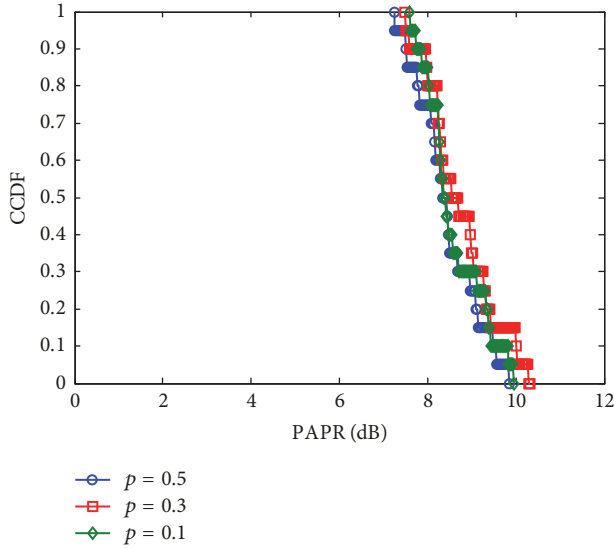


FIGURE 5: Diagram of the CCM-based OFDM system.

FIGURE 6: PAPRs of the CCM-based OFDM system for different p .

signal caused by many identical elements of \mathbf{X} is efficiently restrained in the CCM-based OFDM system. As source sparsity becomes small, it will increase the number of the zero RP symbols. Then, in the case of sparse source, it does not cause high PAPR in the CCM-based OFDM system. Figure 6 depicts the PAPR in the CCM-based OFDM system for different p with $w = \{\pm 1, \pm 2, \pm 4, \pm 4\}$, $M = 480$, $N = 128$, and $L = 8$.

From Figure 6, it can be seen that the PAPR of the CCM-based OFDM system is not sensitive to the source sparsity. As source becomes sparse, it will not bring additional PAPR increase.

4. Performance Evaluation

In the traditional OFDM system and the proposed CCM-based OFDM system, we adopt the SOICF method to evaluate the PAPR reduction performance for different source sparsity. Furthermore, the BER performance is evaluated for different source sparsity over the Additive White Gaussian Noise (AWGN) channel.

For a traditional OFDM system, we consider that it takes QPSK bit-to-symbol mapping operation and 128 subcarriers [20]. For the proposed CCM-based OFDM system, we consider that the size of its generator matrix \mathbf{G} is 1920 rows

and 480 columns [21]. Since the PAPRs with different weight sets are similar, we take the weight set $w = \{\pm 1, \pm 2, \pm 4, \pm 4\}$ with high achievable transmission rate to evaluate the PAPR reduction and BER performance. For source sparsity, we consider the source sparsity p to be 0.5, 0.3, and 0.1 [21]. For the SOICF method, we define A_{th} as the predefined threshold and $\gamma = A_{th}/\sqrt{P_{av}}$ as the clipped ratio and set $\gamma = 2.1$ dB, where P_{av} means the average power of the signals before clipping. The oversampling factor $L = 8$ is able to provide a sufficiently accurate approximation of the PAPR [24], and thus we set $L = 8$ in our simulations.

The PAPR reduction performances are, respectively, shown in Figures 7(a), 7(b), and 7(c) for various source sparsity. Specifically, when the source is nonsparse, for example, $p = 0.5$, the PAPR reduction performances are almost identical in the traditional system and proposed system; when the source becomes sparse, for example, $p = 0.3$ and $p = 0.1$, due to the much higher PAPR for sparse source, the traditional OFDM system fails to restrain its PAPR. However, in the CCM-based OFDM system, because the PAPR of its signals has not been influenced by sparse source, it still can obtain much lower PAPR, and there is a performance gap around 9 dB between two systems when p is 0.1.

Figure 8 shows the BER curves for different OFDM systems and source sparsity after 3 iterations of SOICF. As illustrated in Figure 8, the proposed OFDM system almost has the same BER performance as the traditional OFDM system with nonsparse source. Due to signal distortion caused by PAPR reduction, the BER performance of the traditional OFDM system begins to degrade as source becomes sparse, and the deterioration is about 2 dB at $p = 0.1$. However, in the proposed OFDM system, the BER performance is improved by the channel protection of CCM scheme, and the BER performance becomes better as source becomes sparser. Particularly, the proposed OFDM system outperforms about 4 dB over the traditional OFDM system, when source sparsity is 0.1. In addition, in the case of $w = \{\pm 1, \pm 2, \pm 4, \pm 4\}$, $M = 480$, and $p = 0.1$, the proposed system is able to achieve 8.5 bit/s/Hz average rate and about 12 bit/s/Hz peak rate for seamless rate adaptation [21].

5. Conclusion

In this paper, we have presented CCM-based OFDM system to reduce PAPR for sparse source. By using the CCM scheme in the traditional OFDM system, the generated frequency OFDM symbols are concentrated in zero, and the sparser

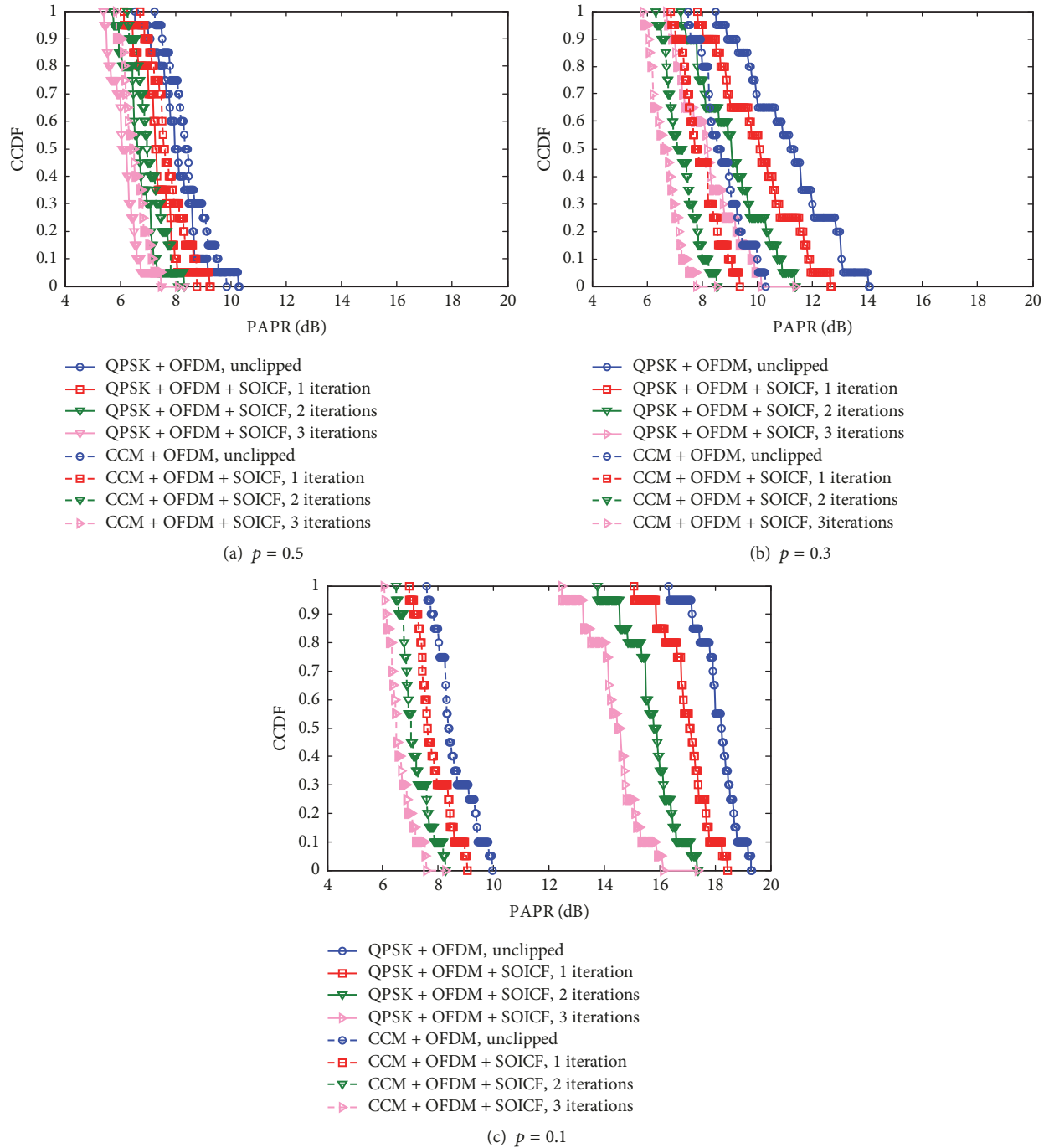


FIGURE 7: PAPR reduction with different source sparsity and iterations.

the source is, the more zero symbols there are. The zero symbols will not bring additional PAPR increase. Thus, the proposed CCM-based OFDM system, together with iterative clipping and filtering, can efficiently restrain the high PAPR for sparse source. Finally, the simulation results show that the proposed OFDM system almost has the same performance in terms of PAPR reduction as the traditional OFDM system regardless of source sparsity. Moreover, the BER performance of the proposed OFDM system is improved by the use

of CCM scheme. Particularly, the proposed OFDM system outperforms about 4 dB over the traditional OFDM system when source sparsity is 0.1. In addition, the proposed CCM-based OFDM system also maintains the characteristic of seamless rate adaptation.

Conflicts of Interest

The authors declare that they have no conflicts of interest.

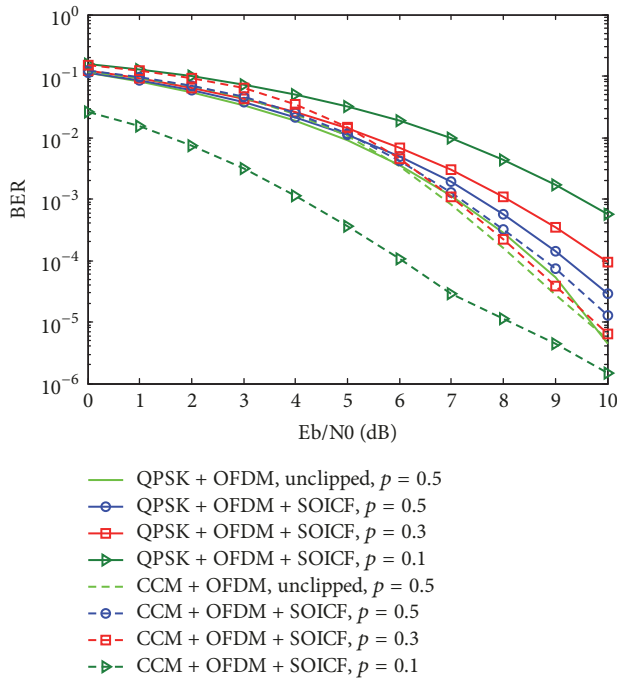


FIGURE 8: BER performance for different source sparsity.

Acknowledgments

This work was supported by the National Natural Science Foundation of China (Grant 61471022) and NSAF (Grant U1530117).

References

- [1] L. J. Cimini, "Analysis and simulation of a digital mobile channel using orthogonal frequency division multiplexing," *IEEE Transactions on Communications*, vol. 33, no. 7, pp. 665–675, 1985.
- [2] J. A. C. Bingham, "Multicarrier modulation for data transmission: an idea whose time has come," *IEEE Communications Magazine*, vol. 28, no. 5, pp. 5–14, 1990.
- [3] C. Ru, L. Yin, J. Lu, and C. W. Chen, "UEP video transmission based on dynamic resource allocation in MIMO OFDM system," in *Proceedings of the 2007 IEEE Wireless Communications and Networking Conference, (WCNC '07)*, pp. 310–315, China, March 2007.
- [4] I. Koffman and V. Roman, "Broadband wireless access solutions based on OFDM access in IEEE 802.16," *IEEE Communications Magazine*, vol. 40, no. 4, pp. 96–103, 2002.
- [5] Z. Fei, C. Xing, N. Li, Y. Han, D. Danev, and J. Kuang, "Power allocation for OFDM-based cognitive heterogeneous networks," *Science China Information Sciences*, vol. 56, no. 4, pp. 1–10, 2013.
- [6] Z. Chen, L. Yin, Y. Pei, and J. Lu, "CodeHop: physical layer error correction and encryption with LDPC-based code hopping," *Science China Information Sciences*, vol. 59, no. 10, Article ID 102309, 2016.
- [7] P. Wang, L. Yin, and J. Lu, *An efficient helicopter-satellite communication scheme based on check-hybrid ldpc coding*, *Tsinghua science and technology*, 2018.
- [8] J. Joung, C. K. Ho, K. Adachi, and S. Sun, "A survey on power-amplifier-centric techniques for spectrum- and energy-efficient wireless communications," *IEEE Communications Surveys & Tutorials*, vol. 17, no. 1, pp. 315–333, 2015.
- [9] G. Wunder, R. F. H. Fischer, H. Boche, S. Litsyn, and J.-S. No, "The PAPR problem in OFDM transmission: new directions for a long-lasting problem," *IEEE Signal Processing Magazine*, vol. 30, no. 6, pp. 130–144, 2013.
- [10] Y. Rahmatallah and S. Mohan, "Peak-to-average power ratio reduction in ofdm systems: a survey and taxonomy," *IEEE Communications Surveys & Tutorials*, vol. 15, no. 4, pp. 1567–1592, 2013.
- [11] J. Ji, G. Ren, and H. Zhang, "PAPR reduction of sc-fdma signals via probabilistic pulse shaping," *IEEE Transactions on Vehicular Technology*, vol. 64, no. 9, pp. 3999–4008, 2015.
- [12] S.-H. Wang, W.-L. Lin, B.-R. Huang, and C.-P. Li, "PAPR reduction in OFDM systems using active constellation extension and subcarrier grouping techniques," *IEEE Communications Letters*, vol. 20, no. 12, pp. 2378–2381, 2016.
- [13] H. Wang, X. Wang, L. Xu, and W. Du, "Hybrid PAPR reduction scheme for FBMC/OQAM systems based on multi data block PTS and TR methods," *IEEE Access*, vol. 4, no. 99, pp. 4761–4768, 2016.
- [14] S. Shu, D. Qu, L. Li, and T. Jiang, "Invertible subset QC-LDPC codes for PAPR reduction of ofdm signals," *IEEE Transactions on Broadcasting*, vol. 61, no. 2, pp. 290–298, 2015.
- [15] J. Armstrong, "Peak-to-average power reduction for OFDM by repeated clipping and frequency domain filtering," *IEEE Electronics Letters*, vol. 38, no. 5, pp. 246–247, 2002.
- [16] L. Wang and C. Tellambura, "A simplified clipping and filtering technique for PAR reduction in OFDM systems," *IEEE Signal Processing Letters*, vol. 12, no. 6, pp. 453–456, 2005.
- [17] R. J. Baxley, C. Zhao, and G. T. Zhou, "Constrained clipping for crest factor reduction in OFDM," *IEEE Transactions on Broadcasting*, vol. 52, no. 4, pp. 570–575, 2006.
- [18] J. Tong, L. Ping, Z. Zhang, and V. K. Bhargava, "Iterative soft compensation for OFDM systems with clipping and superposition coded modulation," *IEEE Transactions on Communications*, vol. 58, no. 10, pp. 2861–2870, 2010.
- [19] Y.-C. Wang and Z.-Q. Luo, "Optimized iterative clipping and filtering for PAPR reduction of OFDM signals," *IEEE Transactions on Communications*, vol. 59, no. 1, pp. 33–37, 2011.
- [20] X. Zhu, W. Pan, H. Li, and Y. Tang, "Simplified approach to optimized iterative clipping and filtering for PAPR reduction of OFDM signals," *IEEE Transactions on Communications*, vol. 61, no. 5, pp. 1891–1901, 2013.
- [21] H. Cui, C. Luo, J. Wu, C. W. Chen, and F. Wu, "Compressive coded modulation for seamless rate adaptation," *IEEE Transactions on Wireless Communications*, vol. 12, no. 10, pp. 4892–4904, 2013.
- [22] T. Jiang, M. Guizani, H.-H. Chen, W. Xiang, and Y. Wu, "Derivation of PAPR distribution for OFDM wireless systems based on extreme value theory," *IEEE Transactions on Wireless Communications*, vol. 7, no. 4, pp. 1298–1305, 2008.
- [23] G. Caire, S. Shamai, A. Shokrollahi, and S. Verdù, "Fountain codes for lossless data compression," in *DIMACS Series in Discrete Mathematics and Theoretical Computer Science*, vol. 68, pp. 1–18, 2005.
- [24] C. Tellambura, "Computation of the continuous-time PAR of an OFDM signal with BPSK subcarriers," *IEEE Communications Letters*, vol. 5, no. 5, pp. 185–187, 2001.

